BIOCHEMISTRY
including biophysical chemistry & molecular biology

Article

pubs.acs.org/biochemistry

PatA and PatB Form a Functional Heterodimeric ABC Multidrug Efflux Transporter Responsible for the Resistance of *Streptococcus pneumoniae* to Fluoroquinolones

Emilie Boncoeur,[†] Claire Durmort,[†] Benoît Bernay,[†,§] Christine Ebel,[†] Anne Marie Di Guilmi,[†] Jacques Croizé,[‡] Thierry Vernet,*[,†] and Jean-Michel Jault*[,†]

[†]Université Joseph Fourier-Grenoble 1, Institut de Biologie Structurale, Grenoble, France, CNRS, Institut de Biologie Structurale, Grenoble, France, and CEA, Institut de Biologie Structurale, Grenoble, France

[‡]Unité de bactériologie, CHU la Tronche, Grenoble, France

ABSTRACT: All bacterial multidrug ABC transporters have been shown to work as either homodimers or heterodimers. Two possibly linked genes, *patA* and *patB* from *Streptococcus pneumococcus*, that encode half-ABC transporters have been shown previously to be involved in fluoroquinolone resistance. We showed that the Δ*patA*, Δ*patB*, or Δ*patA*/Δ*patB* mutant strains were more sensitive to unstructurally related compounds, i.e., ethidium bromide or fluoroquinolones, than the wild-type R6 strain. Inside-out vesicles prepared from *Escherichia coli* expressing PatA and/or PatB transported Hoechst 33342, a classical substrate of multidrug transporters, only when both PatA and PatB were coexpressed. This transport was inhibited either by orthovanadate or by reserpine, and mutation of the conserved Walker A lysine residue of either PatA or PatB fully abrogated Hoechst 33342 transport. PatA, PatB, and the PatA/PatB heterodimer were purified from detergent-solubilized *E. coli* membrane preparations. Protein dimers were identified in all cases, albeit in different proportions. In contrast to the PatA/PatB heterodimers, homodimers of PatA or PatB failed to show a vanadate-sensitive ATPase activity. Thus, PatA and PatB need to interact together to make a functional drug efflux transporter, and they work only as heterodimers.

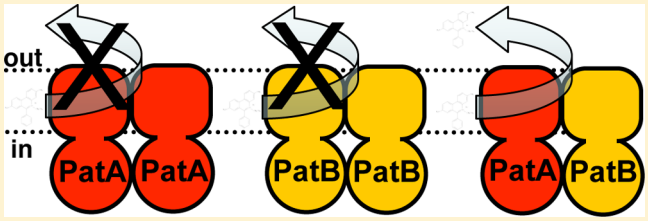

Streptococcus pneumoniae (the pneumococcus) is one of the most severe human Gram-positive pathogens with frequent deadly outcomes in young children, immunocompromised patients, and elderly people (~1.6 million death/year worldwide according to the World Health Organization).[1] In addition, multidrug resistance (MDR) *S. pneumoniae* strains are spreading rapidly and pose a serious health threat.[2] Although antibiotic resistance can have a multifaceted origin, multidrug transporters have drawn much attention lately because of their major involvement in the resistance of pathogenic microorganisms to drug treatment.[3,4] Multidrug transporters are found in all living organisms and can use either ions or ATP as the energy source. Multidrug transporters powered by ATP belong to the largest family of membrane proteins, the ABC (ATP-binding cassette) family.[5] Members of this family involved in MDR phenotypes are found from bacteria to humans, and the most prominent example, the P-glycoprotein (Pgp or ABCB1), is involved in the resistance of cancer treatments.[6] ABC transporters share a common basic architecture, with two hydrophilic nucleotide-binding domains (NBDs) that hydrolyze ATP to energize the transporter and two transmembrane domains (TMDs) that drive the translocation of the substrate across the membrane.[7,8] These four domains are either fused into a single polypeptide (full transporters, e.g., Pgp) or borne from two to four separate polypeptides. In bacteria, all multidrug ABC transporters identified so far have one NBD genetically fused to one TMD.[9−17] Thus, they work as homodimers or heterodimers and are called half-transporters.[18]

Through systematic inactivation of genes encoding putative drug efflux transporters in the virulent strain of *S. pneumoniae* TIGR4, Robertson et al. reported the first genetic evidence that the half-ABC transporters SP2073 (PatB) and SP2075 (PatA) presumably function together to confer intrinsic resistance to structurally unrelated compounds, including some fluoroquinolones.[19] Overexpression of these two genes was also reported in ciprofloxacin-resistant or linezolid-resistant laboratory-selected mutants,[20,21] as well as in clinical isolates.[22] Overall, these reports implicate these two half-ABC transporters in pneumococcal resistance to multiple antibiotics and infer their in vivo heterodimerization. Intriguingly, though, the formation of homodimers of PatA was also envisioned to explain the resistance of a mutant strain to reserpine.[23] Thus, the functional molecular organization of the PatA/PatB system remains unclear.

In this report, we first reassessed the effect of the deletion of *patA*, *patB*, and *patA*/*patB* on the growth of *S. pneumoniae* strain R6 because contradictory results were reported in the literature depending upon the background wild type used.[19,21]

Received: June 8, 2012
Revised: September 4, 2012
Published: September 5, 2012

Then, to shed light on the functioning mechanism of PatA and PatB, we overexpressed these two proteins either alone or jointly in *Escherichia coli*. Using inside-out vesicles, a drug transport and a high vanadate-sensitive ATPase activity were observed only when both proteins were coexpressed. To address the question of the oligomerization status of the PatA/PatB system, both proteins were detergent-solubilized, purified, and characterized either alone or in combination. Although PatA was able to homodimerize, as was PatB but to a lesser extent, neither homodimer displayed drug transport or ATPase activity contrary to the heterodimer. Therefore, our results demonstrate that PatA−PatB association is required in vitro for the formation of a functional multidrug efflux transporter, a situation likely to prevail in the pneumococcus

EXPERIMENTAL PROCEDURES

Bacteria and Growth Conditions. *S. pneumoniae* genomic DNA from strain R6 was used for *patA* and *patB* amplification. *E. coli* Top 10 (Invitrogen) and *E. coli* C41(DE3) strains[24] were used for gene cloning and protein overexpression, respectively. *S. pneumoniae* were grown in Bacto Todd Hewitt Broth (TH broth) (Difco) at 37 °C under 5% CO_2 in air, and *E. coli* strains were grown in Luria-Bertani (LB) or Turbo Broth (TB) (AthenaES) at 37 °C.

Construction of Δ*patA*, Δ*patB*, or Δ*patA*/Δ*patB* Mutants of *S. pneumoniae*. Deletion of the *patA* or *patB* gene from wild-type (WT) strain R6 was done as previously described.[25] Briefly, cassettes encoding the choramphenicol (CAT) or kanamycin (KAN) antibiotic resistance genes were used to replace the *patA* or *patB* gene, respectively. Plasmid pR326[26] or pCEP[27] was used as a template to amplify the sequence of the CAT or KAN resistance gene, respectively, flanked with either *patA* or *patB* sequences. The newly synthesized DNA containing either the CAT or KAN gene was transformed into competent *S. pneumoniae* R6 strains. Mutant strains without the *patA* or *patB* gene were isolated by two successive platings on antibiotic plates containing 5 μg/mL CAT or 500 μg/mL KAN. The following polymerase chain reaction (PCR) primers were used: for *patA*, 5′CCCAATCCCAGTAACCGTCG, 3′TCAAACAAATTTTCATCAAGCTTGCTTGAACTAAATTGGCTAGC, 5′GCTAGCCAATTTAGTTCAAGCAAGCTTGATGAAAATTTGTTTGA, 3′GCAATGACGAAACTAGTTCTACCTCTAGAACTAGTGGATCCCCCGG, 5′CCGGGGGATCCACTAGTTCTAGAGGTAGAACTAGTTTCGTCATTGC, and 3′CAACTGACTCATCACCAACAGG; for *patB*, 5′CGGTATCCATGTTGCCAAGATTGC, 3′AAACGGATCCCACTAGTCCCGACTTCCTGCAGATAACGCGG, 5′CCGCGTTATCTGCAGGAAGTCGGGACTAGTGGGATCCGTTT, 3′GCACCAAGCGCTCTGATTTGGCTTTCAGTTTCGCGATGACAC, 5′GTGTCATCGCGAAACTGAAAGGCCAAATCAGAGCGCTTGGTGC, and 3′CAATGTAGCCATCATCCACC. A combination of these primers was used to create the double mutant, Δ*patA*/Δ*patB*.

Growth of *S. pneumoniae* Wild-Type and Mutant Strains and Determination of Drug Sensitivity. The growth of *S. pneumoniae* strains was assessed using a previously described protocol.[28] TH broth was inoculated with 1/100 *S. pneumonie* cultures grown to logarithmic phase. Cultures (300 μL) were grown in triplicate in 96-well plates sealed with a transparent film. Plates were incubated at 37 °C in a FLUOstar Optima instrument (BMG Labtech). Growth was monitored by recording the turbidity at OD_{600} every 20 min for 17 h and after a 5 s orbital shaking (300 rpm). Drug sensitivity was assessed by adding various concentrations of different drugs in the culture wells as mentioned. The generation time under each condition was calculated from linear phase of the semilog plots corresponding to the log-to-log transition part of the curve using GraphPad Prism. Differences in average generation time between groups were assessed for statistical significance using the unpaired Student's *t* test.

Determination of the Susceptibility of Δ*patA*, Δ*patB*, or Δ*patA*/Δ*patB* Mutant Strains to Different Xenobiotics. The susceptibility of each strain to a large panel of xenobiotics has been tested using disk diffusion assays. The wild-type *S. pneumoniae* or Δ*patA*, Δ*patB*, or Δ*patA*/Δ*patB* mutant strains were plated at an OD_{600} of 0.3 on Muller-Hinton blood agar plates, and a filter paper disk impregnated with 100 μL of xenobiotics at various concentrations was applied to the agar surface. Each plate was incubated overnight at 37 °C, under 5% CO_2. The susceptibility of each mutant strain to xenobiotics was determined by the measurement of the growth inhibitory halo around the disk and compared to that of the wild-type strain.

Construction of *patA*, *patB*, and *patA*/*patB* Plasmids for Recombinant Protein Expression and Site-Directed Mutagenesis. Genomic DNA from *S. pneumoniae* strain R6 was used as a template to amplify the sequence of either the *patA* or *patB* gene with the Phusion polymerase (Ozyme). *patA* and *patB* were cloned into a pETDuet vector using a combination of SacI/NotI and NdeI/XhoI restriction sites, respectively. By doing so, we fused *patA* in frame with a sequence encoding a His tag sequence coming from the vector. To also provide a six-histidine tag at the N-terminus of the PatB protein, we added an additional sequence encoding six histidine residues by PCR to the *patB* fragment during the amplification step. Thus, both PatA and PatB, when overexpressed from this pETDuet-PatA/PatB plasmid, contained a His tag at their N-termini. *patA* or *patB* alone was introduced in the first multicloning site of the pETDuet, and therefore, they each contained a His tag at their N-termini. Plasmid constructs were verified by DNA sequencing (Cogenics). The QuickChange Site-Directed Mutagenesis Kit (Stratagene) was used to insert a single mutation into PatA (Lys388Ala or PatA*) or PatB (Lys367Ala or PatB*). The pETDuet/*patA* Lys388Ala/*patB* Lys367Ala double mutant (or PatA*/PatB*) was obtained by using either pETDuet/*patA* Lys388Ala/*patB* or the pETDuet/*patA*/*patB* Lys367Ala as a template. The following primers were used: for PatA, 5′GAGCTCGAAGACAGTTCAATTTTTTTGGCATTATTTTAAG and 3′GCGGCCGTTCGAAAACAAATTGATTGTGATAGAGTTCTG; for PatB, 5′ATATGCATCACCATCATCACCACCTGATTCAGAAAATAAAAACCTACAAGTGGCAG and 3′CTCGAGTCATTTCTGTGTTTCATAGATTTCACGGTAAAC.

To introduce the Walker A mutation, the following primers were used: 5′GACCGGTTCAGGAGCAACGACTATTATG for PatA and 5′GCGACTGGTGCAGGAGCGTCGACCTTAGCTCAATTGATTCC for PatB (with a concomitant introduction of AgeI and SalI restriction sites, respectively, to screen for positive clones). The correct DNA sequences were verified by DNA sequencing (Beckman Coulter Genomics).

Protein Overexpression and Inside-Out Membrane Vesicle (IMV) Preparation. Freshly transformed C41(DE3) *E. coli* (no close homologues to *patA* or *patB* are present in the genome) colonies were inoculated into TB and grown at 37 °C

while being shaken at 200 rpm. At an OD_{600} of 1.8, 0.7 mM isopropyl β-D-thiogalactopyranoside (IPTG) was added. The culture was further grown overnight at 25 °C, and bacteria were collected by low-speed centrifugation (5000*g* for 20 min). Subsequent bacterial lysis and IMV preparation were conducted as previously described,[14] except that a microfluidizer was used instead of the French press and cells were broken by three passages at 18000 psi. Protein overexpression was checked by Coomassie brilliant blue-stained sodium dodecyl sulfate−polyacrylamide gel electrophoresis (SDS−PAGE).

Fluorescent Drug Transport and Ethidium Bromide (EtBr) Incorporation. For drug transport assays, fluorescence changes were monitored with a Photon Technology International Quanta Master I fluorimeter essentially as previously described.[29] Excitation and emission wavelengths were set at 355 and 457 nm, respectively, for Hoechst 33342 [2′-(4-ethoxyphenyl)-5-(4-methyl-1-piperazinyl)-2,5′-bis-1*H*-benzimidazole (Sigma)]. Briefly, inside-out membrane vesicles (IMVs) (200 μg of protein) were added to a 2 mL cuvette containing 1 mL of 50 mM Hepes-KOH (pH 8.0), 2 mM $MgCl_2$, 8.5 mM NaCl, 40 μg of pyruvate kinase (Roche), and 4 mM phosphoenolpyruvate. After incubation for 1 min at 25 °C, the drug was added, and its fluorescence was recorded for 1−2 min. ATP (2 mM) was then added, and the fluorescence intensity was monitored for several minutes. Reserpine, orthovanadate, and AMP-PNP (Sigma Aldrich) were used when indicated. For the transport of EtBr in whole bacteria, *S. pneumoniae* WT or Δ*patA*, Δ*patB*, or double mutant Δ*patA*/Δ*patB* knockout strains were grown for 6 h in TH until the OD_{600} reached 0.3. Bacteria were pelleted and resuspended in 0.35 M NaCl. Then, 270 μL of the sample was mixed with 730 μL of transport buffer [50 mM KP_i (pH 7.2), 25 mM glucose, and 5 mM $MgSO_4$] and transferred into a fluorometer cuvette. Upon addition of 10 μM EtBr, the fluorescence was recorded at 25 °C. The excitation and emission wavelengths used were 500 and 580 nm, respectively.

Purification of PatA, PatB, and the PatA/PatB Heterodimer (PatA/PatB). IMVs containing overexpressed PatA, PatB, or PatA/PatB were solubilized for 2 h on ice in buffer A [50 mM Tris-HCl (pH 8), 15% glycerol, 100 mM NaCl, and 5 mM β-mercaptoethanol] containing 10 mM imidazole and 1% *N*-dodecyl β-D-maltoside (DDM) at a protein concentration of 2−5 mg/mL. After centrifugation for 1 h at 50000*g*, the supernatant was incubated with a 1/10 (v/v) dilution of Ni^{2+}-NTA resin (Qiagen) for 1 h. The slurry was poured into a column, and the resin was washed with 20 column volumes of buffer A containing 0.05% DDM and 20 mM imidazole. Elution was conducted in the same buffer but in the presence of 250 mM imidazole. Purified proteins were dialyzed against 50 mM Tris-HCl (pH 8), 50 mM NaCl, 10% (v/v) glycerol, 5 mM β-mercaptoethanol, and 0.05% DDM. All steps were conducted at 4 °C or on ice. Purified proteins were flash-frozen in liquid N_2 and stored at −80 °C. The protein concentration was determined using the Bradford assay (Coomassie Blue, Pierce) or by measuring the OD_{280} using a NanoDrop 2000c instrument (Thermo Scientific) according to the manufacturer's recommendations.

Analytical Ultracentrifugation. Purified proteins were first subjected to gel filtration on Sephadex G200 in 50 mM Tris-HCl (pH 8), 50 mM NaCl, 10% (v/v) glycerol, and 0.05% DDM, concentrated on an Amicon filter (50 kDa molecular mass cutoff), and frozen at 4 °C before sedimentation velocity experiments were conducted. Similar results were obtained with unfrozen samples (data not shown). Sedimentation velocity experiments were performed on an XLI Beckman ultracentrifuge, at 10 °C and 42000 rpm, using an AnTi 50 rotor and two-channel centerpieces equipped with sapphire windows and filled with a detergent-free solvent in the reference compartment. Data were acquired using interference optics and absorbance optics at 280 nm at time intervals of typically 12 min, and the $c(s)$ analysis of Sedfit was used for data analysis.[30] We estimated the buoyant molecular mass (M_b) of the protein−detergent complexes by combining sedimentation coefficient s with hydrodynamic radius R_H deduced from calibrated size exclusion chromatography using the relationship $M_b = 6\pi N_a \eta R_H s$, where η is the solvent viscosity and N_a is Avogadro's number. M_b is related to the protein molecular mass and partial specific volume, M_P and $\overline{v}_P$, respectively, detergent binding in grams per gram and partial specific volume, B and $\overline{v}_D$, respectively, and solvent density, ρ $\{M_b = M_P[(1 - \rho\overline{v}_P) + B(1 - \rho\overline{v}_D)]\}$. We calculated the frictional ratio f/f_{min} as the ratio R_H/R_{min}, with R_{min} being the radius of the anhydrous volume of the complexes defined from its composition and partial specific volume. Details and theoretical background are given in refs 31−33. Using Sednterp (http://www.jphilo.mailway.com/), we calculated from the amino acid sequences of PatA, PatB, and PatA/PatB molecular masses of 67368, 62194, and 129544 kDa, partial specific volumes of 0.743, 0.747, and 0.745 mL/g (at 10 °C), and extinction coefficients at 280 nm of 0.643, 0.754, and 0.696 L g^{-1} cm^{-1}, respectively. A refractive index increment ($\partial n/\partial c$) of 0.187 g/mL was used for the proteins. For DDM, a partial specific volume of 0.82 mL/g and a $\partial n/\partial c$ of 0.143 g/mL were used.[30] A solvent density of 1.026 g/mL and a viscosity of 1.75 cP were extrapolated from published values measured at 20 °C.[34] The calculation from the sedimentation coefficients (s_{exp}) of the corrected values ($s_{20,w}$) was conducted using a partial specific volume for the protein−DDM complex of 0.78 mL/g.

Size Exclusion Chromatography Coupled to Light Scattering (SEC−LS) Experiments. Aliquots (20 μL) recovered from the gel filtration (see above) were also injected at a flow rate of 0.5 mL/min into a high-pressure liquid chromatography system (LC20 AD, Shimadzu) in a KW 803 column (8 mm × 300 mm) preceded by a guard column (Shodex) previously equilibrated at 10 °C with a buffer filtered at 0.1 μm containing 50 mM Tris-HCl (pH 8), 50 mM NaCl, 5 mM β-mercaptoethanol, and 0.05% DDM. The elution profile was followed online by refractive index (Δn) measurements with an Optilab rEX instrument (Wyatt Technology), absorbance at 250 nm (A_{250}) with a Shimadzu SPD-M20A instrument, and light scattering intensity (I) with a miniDAWN TREOS detector (Wyatt Technology) using a laser emitting at λ_0 = 658 nm. Data were analyzed using ASTRA (Wyatt Technology). The basic equation for light scattering, restricted to diluted solutions of small particles (R_H < 20 nm), reduces to $I = KcM \times (\partial n/\partial c)^2$, where I is the excess intensity of scattered light, K is an optical parameter, c is the concentration, and $\partial n/\partial c$ is the refractive index increment.[31,32] The combination of the A_{250} and Δn signals allows in principle the determination of the composition in terms of protein and detergent within the complexes. From their amino acid composition and using Sednterp, we obtained extinction coefficients at 250 nm for PatA, PatB, and PatA/PatB of 0.270, 0.330, and 0.299 L g^{-1} cm^{-1}, respectively. This analysis was not appropriate (see the text), and molecular masses for the entire complexes were determined using the concentrations derived from the refractive

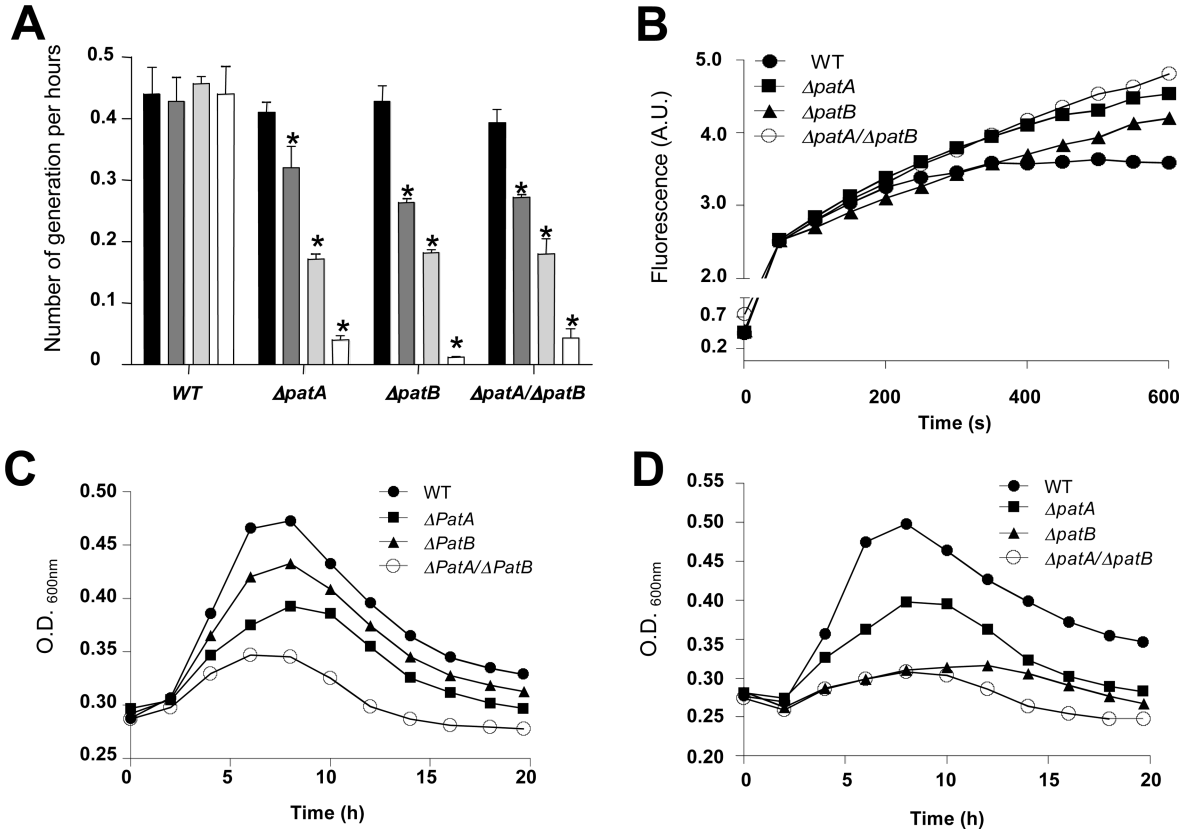

Figure 1. PatA and PatB are required to transport EtBr and confer pneumococcus resistance to xenobiotics. (A) Impact of increasing concentrations of EtBr on the growth of wild-type *S. pneumoniae* or Δ*patA*, Δ*patB*, or Δ*patA*/Δ*patB* mutant strains: (black bars) no EtBr, (dark gray bars) 0.025 μg/mL EtBr, (light gray bars) 0.05 μg/mL EtBr, and (white bars) 0.1 μg/mL EtBr. The generation time of each strain was obtained by measuring the slopes of the exponential growth phases. A histogram representative of three independent experiments in duplicate is shown, Error bars represent the standard error of the mean. Significance was determined by a *t* test. *$p < 0.05$ ($n = 3$). (B) Incorporation of EtBr into *S. pneumoniae* R6 WT (●) or Δ*patA* (■), Δ*patB* (▲), and Δ*patA*/Δ*patB* (○) mutant strains. Three independent experiments were performed, and typical results obtained in one of these experiments are shown here. (C and D) Impact of 100 ng/mL ciprofloxacin (C) and 400 ng/mL norfloxacin (D) on the growth profile of wild-type *S. pneumoniae* (●) or Δ*patA* (■), Δ*patB* (▲), and Δ*patA*/Δ*patB* (○) mutant strains. The graph represents the growth curve profile of each strain co-incubated with ciprofloxacin or norfloxacin. Three independent experiments were performed, and typical results obtained in one of them are shown here.

index measurements with a $\partial n/\partial c$ of 0.165 g/mL intermediate between protein and DDM. Hydrodynamic radii (R_H) were estimated from the elution volume, after calibration with ribonuclease, carbonic anhydrase, bovine serum albumin, conalbumin, catalase, and thyroglobulin (R_H values of 1.364, 2.3, 3.55, 4.0, 5.22, and 8.5 nm, respectively).

Determination of ATPase Activity. ATPase activities were measured using an enzymatic assay that allows ATP regeneration coupled to NADH oxidation, which is followed in real time at 340 nm with a UVmc^2 Safas spectrophotometer.[35] For proteins in detergent (20−50 μg), ATPase activities were measured at 30 °C in dialysis buffer supplemented with 32 μg/mL lactate dehydrogenase (Roche), 60 μg/mL pyruvate kinase (Roche), 4 mM phosphoenolpyruvate, and 0.4 mM NADH. Increasing amounts of ATP were added from 0.1 to 5 mM. Orthovanadate (Sigma) was prepared at 100 mM as described previously[34] and heated at 95 °C for 5 min before being used. The initial rate of ATP hydrolysis was plotted versus the ATP concentration, and curve fitting was performed using GraFit 5.0 (Erithacus Software).

Statistical Analysis. All data are presented as means ± the standard error of the mean. Comparisons among groups were analyzed by an unpaired Student's *t* test, and factorial analysis of variance with post hoc comparison (Fisher's protected least significant difference). The level of significance was defined to be $p < 0.05$.

RESULTS

Increased Sensitivity of *S. pneumoniae* to Xenobiotics When *patA* or *patB* Genes Are Deleted. Whereas deletion of *patA* was originally reported to have no consequence on the growth of the TIGR4 strain,[19] the same deletion significantly reduced the rate of growth of the R6 strain.[21] Moreover, deletion of *patA* could not be accomplished in the M22 strain, suggesting that *patA* is essential in this genetic background.[21] On the other hand, deletion of *patB* did not significantly alter the growth kinetics regardless of the background strain used.[19,21] Therefore, we first revisited the effect of single or double deletions on the growth of the R6 pneumococcal strain. Neither growth defect (Figure 1A, black bars) nor morphological difference (data not shown) were observed for Δ*patA*, Δ*patB*, and Δ*patA*/Δ*patB* mutant strains. The susceptibility of Δ*patA*, Δ*patB*, or Δ*patA*/Δ*patB* mutant strains to different xenobiotics was then tested using disk diffusion assays. All three mutant strains were more sensitive to acriflavine, ciprofloxacin, and norfloxacin than the wild-type strain (data not shown). To investigate the increased sensitivity of pneumococcus mutants to xenobiotics, the effect of ethidium bromide, a typical

dx.doi.org/10.1021/bi300762p | *Biochemistry* 2012, 51, 7755−7765

substrate of many multidrug efflux pumps, was analyzed on each mutant strain. A reduction in the growth rate of either mutant over the WT was more pronounced as the concentration of EtBr increased (Figure 1A). The highest tested concentration of EtBr (0.1 μg/mL) had no effect on the wild-type growth rate, whereas it caused a marked reduction in the growth rate for the three mutants, up to 20 times for the *patB* mutant. Thus, deletion of *patA*, *patB*, or a combination of both perturbed the growth of the pneumococcus in a similar way in the presence of EtBr. Incorporation and efflux of EtBr were also monitored in a real-time assay in each mutant strain as compared to those of the wild type. Following passive diffusion into bacteria, EtBr exhibits an increase in fluorescence intensity upon DNA binding. As shown in Figure 1B, a fast EtBr uptake was seen in the wild-type strain, which progressively slowed to reach a plateau at ~300 s. At that point, the passive EtBr uptake is presumably in equilibrium with an efflux of EtBr because of active pump(s). On the other hand, in the Δ*patA*, Δ*patB*, and Δ*patA*/Δ*patB* mutant strains, the fluorescence increases steadily and does not reach an equilibrium state within the time frame of the experiment. These data indicate that the efflux of EtBr is constantly outcompeted by passive diffusion uptake in these mutant strains. Thus, this suggests that these mutant strains lack or harbor reduced efflux pumps involved in EtBr detoxification. Next, the WT and mutant strains were exposed to 100 ng/mL ciprofloxacin (Figure 1C) or 400 ng/mL norfloxacin (Figure 1D) for 20 h. In preliminary tests, we checked that these concentrations did not affect WT growth. The growth of the three mutants was impaired in the presence of these two antibiotics, with the Δ*patA*/Δ*patB* double mutant being more affected than each single deletion alone, notably in the presence of ciprofloxacin. Indeed, as the doubling time of the wild-type strain exposed to ciprofloxacin was approximately 2 ± 0.8 h, we observed a doubling time of 3 h for each *patA* and *patB* mutant that reached 5 h for the Δ*patA*/Δ*patB* double mutant.

PatA/PatB Forms a Functional Heterodimeric MDR Transporter. The function and oligomeric status of PatA and PatB were investigated following their expression in *E. coli* and purification from membrane preparations. A high level of expression of each protein was obtained in the C41(DE3) *E. coli* strain when they were expressed individually (Figure 2A). The coexpression of PatA/PatB was also very efficient, and both proteins inserted into the *E. coli* membrane with a remarkably high yield (Figure 2B). Measurements using ImageJ of the relative intensities of the PatA and PatB species in membrane fractions or following purification (see Figure 4) revealed that PatA is stained more efficiently than PatB. Taking this difference into account showed that both proteins were stably expressed at comparable levels. Together, and assuming that every protein in the membrane fraction would be stained similarly by the dye, PatA plus PatB would amount to ~60% of total membrane proteins. Substitution of the invariant lysine residue in the Walker A motif in either PatA (PatA*/PatB), PatB (PatA/PatB*), or both proteins (PatA*/PatB*) did not affect the level of expression (Figure 2B). A substantial ATPase activity [~140 nmol of ATP hydrolyzed min^{-1} (mg of protein)$^{-1}$] was found for membrane vesicles containing PatA/PatB (Figure 2C), and this activity was strongly inhibited by vanadate in a dose-dependent manner (~95% at 1 mM). The ATPase activities of the single-lysine mutants, PatA*/PatB or PatA/PatB*, or the double mutant, PatA*/PatB*, were all greatly impaired (~90%). For PatA or PatB alone, a higher

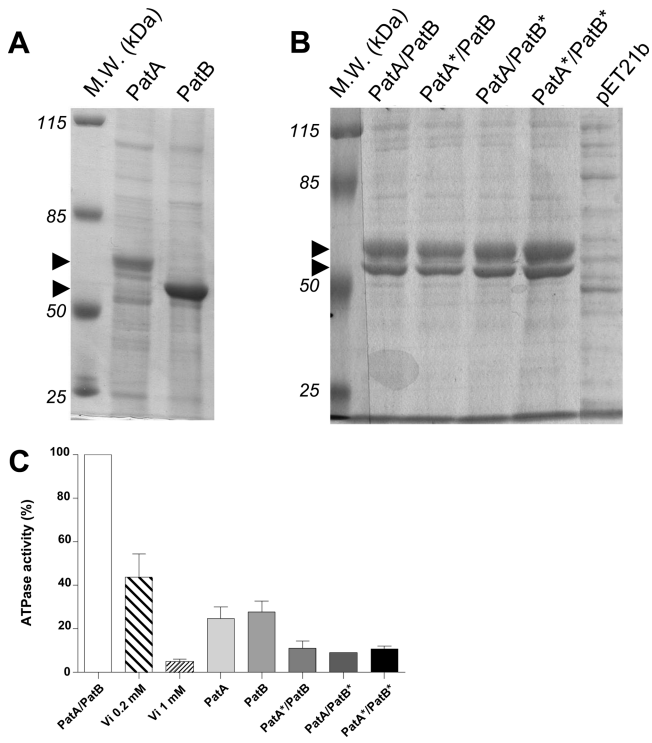

Figure 2. Overexpression of PatA, PatB, and PatA/PatB wild type or mutants and ATPase activities. (A and B) *E. coli* membrane preparations from strains overexpressing PatA, PatB, wild-type PatA/PatB, the Walker A PatA mutant (PatA*/PatB, for K388A), the Walker A PatB mutant (PatA/PatB*, for K367A), or double mutant (PatA*/PatB*) were resolved via 10% SDS−PAGE (10 μg of proteins loaded per lane) and stained with Coomassie blue. A preparation of membrane vesicles made from *E. coli* containing the pET21b vector is shown as a control. The two arrowheads indicate the positions of PatA and PatB. (C) ATPase activities of membrane vesicles containing the different overexpressed proteins as indicated. Orthovanadate (V_i), 0.2 and 1 mM, was added to the PatA/PatB sample. Error bars represent the standard error of the mean for three separate experiments. Under each condition, the *t* test gave a $p < 0.05$.

ATPase activity was detected, amounting to ~20% of that of PatA/PatB. However, it should be noted that a higher level of contaminant in terms of total membrane protein was present in these two preparations, leading possibly to an overestimation of the activity really due to PatA or PatB alone. Alternatively, this ATPase activity might be due to some homodimerization of each half-ABC transporter, and this possible feature is addressed below.

The ability of the proteins to transport fluorescent substrates prototypical for multidrug ABC transporters was monitored using inside-out vesicles. Hoechst 33342 is a membrane-permeable dye highly fluorescent in a membrane environment but poorly fluorescent in aqueous medium. This property allows us to monitor the Hoechst transport in a real-time fluorescence assay.[36,37] Transport of the fluorophore into the lumen of inside-out vesicles by wild-type PatA/PatB, but not for PatA or PatB alone, was evidenced by a rapid fluorescence decay upon addition of ATP (Figure 3A). To check that the transport by PatA/PatB required ATP binding and hydrolysis, PatA*/PatB, PatA/PatB*, and PatA*/PatB* were tested in the same assay. None of the mutants was active in Hoechst 33342 transport (Figure 3B). Moreover, no transport activity was recorded when vanadate was added to the assay or when ATP

dx.doi.org/10.1021/bi300762p | *Biochemistry* 2012, 51, 7755−7765

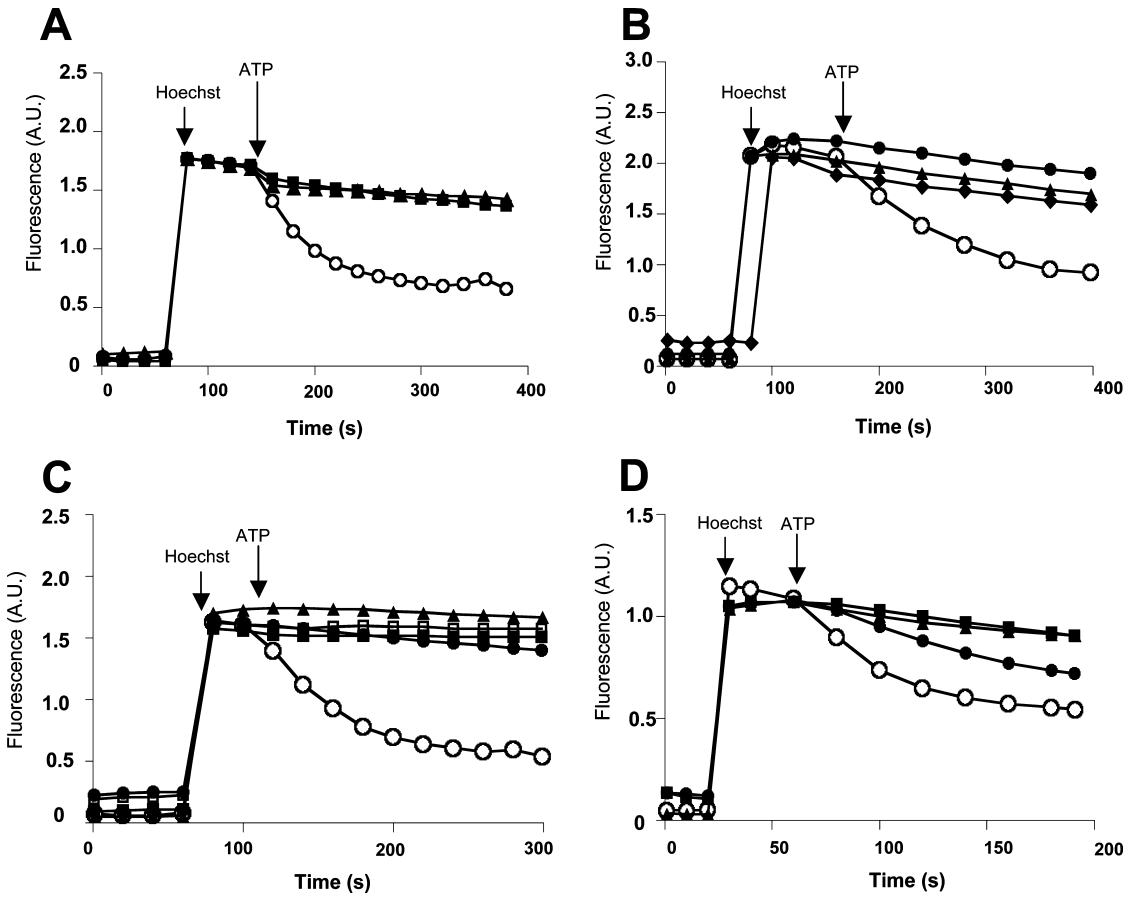

Figure 3. PatA/PatB heterodimers are required to transport the Hoechst 33342 substrate in an active process. (A) Hoechst 33342 (2 μM) was added to 100 μg of inside-out vesicles containing overexpressed PatA/PatB (○), PatA alone (■), or PatB alone (▲), and after ~50 s, 2 mM ATP was added to initiate Hoechst 33342 transport. (B) Hoechst 33342 (2 μM) was added to 100 μg of inside-out vesicles containing overexpressed wild-type PatA/PatB (○), PatA*/PatB (●), PatA/PatB* (▲), or PatA*/PatB* (◆). (C) Hoechst 33342 (2 μM) was added to 100 μg of inside-out vesicles containing overexpressed PatA/PatB with no prior treatment (○) or after a prior addition of 25 μM reserpine (●) or 1 mM orthovanadate (■). As a control, 2 mM AMP-PNP was also used instead of ATP after the addition of 2 μM Hoechst 33342 to 100 μg of inside-out vesicles containing overexpressed PatA/PatB (□). Inside-out vesicles prepared from bacteria containing the pETDuet plasmid alone were also used as another control (▲). (D) Hoechst 33342 (2 μM) was added directly to inside-out vesicles containing overexpressed PatA/PatB (○) or after a prior addition of 2.5 μg/mL norfloxacin (●), 2.5 μg/mL ciprofloxacin (■), or 5 μg/mL EtBr (▲). For each panel, three independent experiments were performed, and typical results obtained in one of these experiments are shown.

was replaced by AMP-PNP, a nonhydrolyzable ATP analogue (Figure 3C). Addition of reserpine, an inhibitor of many multidrug transporters that has been shown to prevent drug efflux by bacterial ABC transporters, including PatA/PatB,[23] also prevented the transport of Hoechst 33342. As a negative control, the absence of measurable transport using inside-out vesicles prepared from *E. coli* transformed with the pET vector confirms that the activities reported above originate from our recombinant transporters and not from endogenous contaminants. To check if the PatA/PatB heterodimers bind ciprofloxacin, norfloxacin, and EtBr, the capacity of these compounds to compete with Hoechst 33342 transport was monitored. As shown in Figure 3D, addition of either ciprofloxacin (2.5 μg/mL), norfloxacin (2.5 μg/mL), or EtBr (5 μg/mL) greatly reduced the Hoechst 33342 transport activity by membrane vesicles containing PatA/PatB. A similar fluorescence assay was used to monitor the transport of other fluorescent substrates.[13,14] Wild-type PatA/PatB, but not the Walker A lysine single or double mutants, was also shown to transport the doxorubicin. Again, addition of vanadate strongly attenuated this transport (data not shown).

Purified PatA and PatA/PatB Are Mainly Dimeric in Contrast to PatB Alone. Membrane fractions containing PatA or PatB alone or PatA/PatB were solubilized in the presence of DDM, a detergent successfully used previously to purify two related ABC transporters from *Bacillus subtilis* overexpressed in *E. coli*.[13,34] The proteins were purified using nickel affinity chromatography. The proteins obtained were essentially homogeneous following this single-affinity purification step (Figure 4A). After purification, a yield of ~0.5 mg/L of culture medium was obtained for PatB and PatA/PatB and a yield of 0.8 mg/L for PatA. The oligomeric state of PatA, PatB, and PatA/PatB was assessed by gel filtration (Figure 4B). PatA and PatA/PatB behaved in a very similar manner with some aggregates that eluted in the void volume (~50 mL), while the bulk of the proteins eluted with an apparent molecular mass compatible with a dimer surrounded by the detergent micelle [~60 mL (see ref 34)]. In the case of PatB, although some proteins eluted with a similar apparent molecular mass (~60 mL) corresponding presumably to a PatB homodimer in a detergent micelle (hereafter called "dimer"), another peak eluted at ~70 mL. This latter peak could possibly correspond to a monomer of PatB with the detergent micelle (hereafter

dx.doi.org/10.1021/bi300762p | *Biochemistry* 2012, 51, 7755−7765

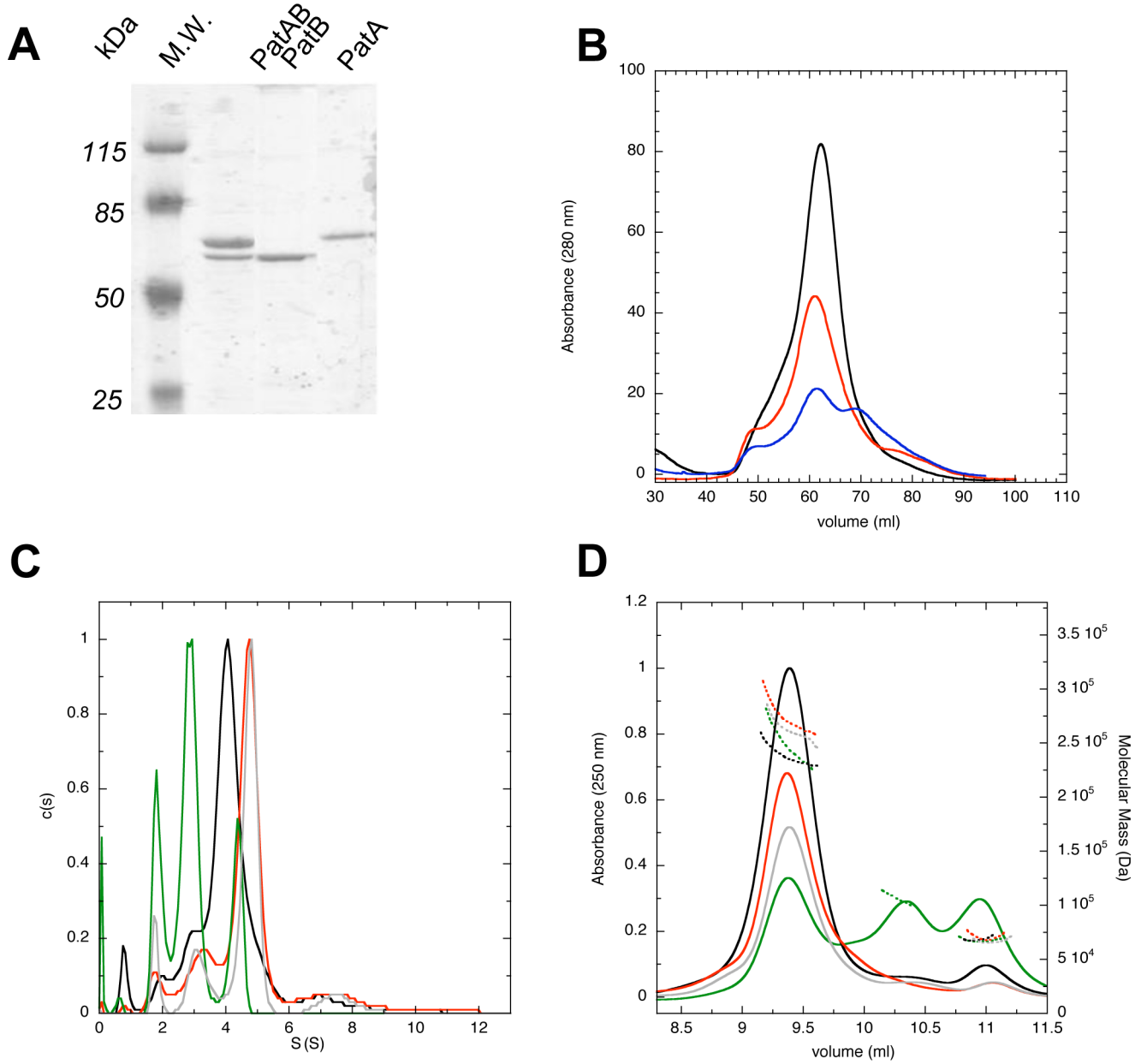

Figure 4. Purification and biochemical characterization of PatA, PatB, and PatA/PatB. (A) SDS−PAGE (10%) stained with Coomassie blue of the fraction eluted from the Ni-NTA column. One to two micrograms of purified proteins was loaded into each lane. (B) Elution profile of PatA (red curve), PatB (blue curve), and PatA/PatB (black curve) from a preparative gel filtration Sephadex G200 column. (C) Samples recovered from the preparative gel filtration in panel B were submitted to a sedimentation velocity experiment using an XLI Beckman ultracentrifuge at 42000 rpm and 10 °C, and the data were measured at 280 nm. The distributions of sedimentation coefficients of PatA (red curve), PatB (monomeric and dimeric fractions, green and gray curves, respectively), and PatA/PatB (black curve) are shown. (D) Samples recovered from the preparative gel filtration in panel B were submitted to size exclusion chromatography on a silica KW 803 column, coupled to light scattering, and elution profiles obtained at 250 nm (left *Y*-axis) and molar masses (right *Y*-axis) of PatA (red curve), PatB (monomeric and dimeric fractions, green and gray curves, respectively), and PatA/PatB (black curve) are shown. The molar masses were estimated for each complex from combined light scattering and refractive index measurements (not shown), using a refractive index increment of 0.165 mL/g. Numerical values are reported in Table 1.

called "monomer"). It should be noted that when the peaks eluting at ∼60 mL and presumably corresponding to the dimeric fraction were further analyzed by SDS−PAGE, the same results as those shown in Figure 4A were obtained, notably for the PatA/PatB sample. Therefore, this particular sample corresponded to a mixture of PatA and PatB that could form heterodimers, but the presence of homodimers of PatA or PatB could not be ruled out. Thus, an in-depth analysis of the different oligomers was performed, first by analytical ultracentrifugation (AUC). Figure 4C shows the results of the sedimentation velocity experiments in terms of $c(s)$ analysis, obtained from the data at 280 nm and using interference optics, the latter emphasizing the detergent contribution. DDM micelles sediment at s = 1.8 S ($s_{20,w}$ = 3.4 S), close to published values.[33] PatA/PatB sediments at s = 4.2 S ($s_{20,w}$ = 8.1 S). PatA and the "dimer" fraction of PatB sediment mainly at 4.7 and 4.8 S ($s_{20,w}$ = 9.1 and 9.3 S, respectively). For these three samples, there is ∼15% of the protein sedimenting slower at $s \approx 3$ S ($s_{20,w} \approx 6$ S) and 15% sedimenting faster at 7−8 S ($s_{20,w} \approx 15$ S). The "monomer" fraction of PatB has a different behavior,

dx.doi.org/10.1021/bi300762p | *Biochemistry* 2012, 51, 7755−7765

Table 1. Biophysical Characterization of PatA, PatB, PatA/PatB, and Related ABC Transporters

		AUC		SEC	SEC−LS	AUC and SEC				
work[a]	complex	s_{exp}[b] (S)	$s_{20,w}$[c] (S)	R_H[d] (nm)	M[e] (kDa)	M_b[f](kDa)	M[g](kDa)	M_p[h](kDa)	B[i] (g/g)	f/f_{min}[j]
1	PatA/PatB	4.2	8.1	6.2	237	52	259	130	1.0	1.4
1	PatA dimer	4.7	9.1	6.2	272	58	290	135	1.2	1.4
1	PatB dimer	4.8	9.3	6.2	261	59	296	124	1.5	1.3
1	PatB monomer	2.9	5.6	4.6	105	27	133	62	1.2	1.3
2	BmrA dimer	5.1	8.5	5.6		47	244	132	0.9	1.3
3	BmrC/BmrD	5.8	8.5	6.1		53	267	145	0.8	1.4

[a]Legend: 1, this work; 2 and 3, s_{exp} and R_H values taken from refs 38 and 34, respectively, and analyzed as those for PatA, PatB, and PatA/PatB. [b]Experimental sedimentation coefficients obtained at 10, 20, and 20 °C with solvent densities of 1.026, 1.036, and 1.026 g/mL and solvent viscosities of 1.75, 1.46, and 1.33 cP for works 1−3, respectively. [c]Corrected sedimentation coefficients calculated using a common value for the partial specific volume of 0.78 mL/g corresponding to 1 g/g of bound detergent. [d]Hydrodynamic radius from column calibration with proteins with known R_H values. [e]Molecular masses of the complexes estimated by a refractive index increment of 0.165 mL/g corresponding to 1 g/g of bound detergent. [f]Buoyant molecular masses of the complexes from s_{exp} and R_H. [g]Molecular masses of the complexes obtained from M_b and considering a partial specific volume of 0.78 mL/g corresponding to 1 g/g of bound detergent. [h]Molecular masses of the protein from the amino acid composition. [i]Bound detergent in grams per gram of protein from s_{exp}, R_H, and M. [j]Frictional ratio of the complexes.

because more than 70% of the protein sediments at s = 2.9 S ($s_{20,w}$ = 5.6 S) and the remaining 30% sediments as a dimer at 4.8 S ($s_{20,w}$ = 9.3S).

The same samples were also investigated using size exclusion chromatography coupled to different detectors (SEC−LS). Changes in light absorption of the eluate were followed at 250 nm and simultaneously analyzed in terms of changes in the refractive index and light scattered at three angles. The general features are similar to those observed via AUC (Figure 4D). PatA, the "dimer" fraction of PatB and PatA/PatB on one hand, and the "monomer" fraction of PatB, on the other hand, elute mainly at volumes corresponding to R_H values of 6.2 and 4.6 nm, respectively. Evaluation of the amount of bound detergent from the combination of absorbance and refractive index data, in AUC and in SEC−LS, leads to aberrant negative binding of detergent for the dimer and ∼0.5 g/g of bound detergent for the monomer. Presumably, the extinction coefficients of the protein used as the inputs were not correct, and detergent binding could not be assessed accurately in such a way. We thus analyze the SEC−LS data using a mean value for the refractive increment of 0.165 mL/g and derive estimates for the molecular masses of the complexes of 255 and 105 kDa for the putative dimer and monomer, respectively, each in the presence of a detergent micelle. The values were within the expected range. They correspond to a detergent binding in the range of 0.5−1 g/g, for the dimer and monomer of 130 and 65 kDa, respectively. We also combined the $s_{20,w}$ and R_H values, from AUC and SEC, to derive buoyant molecular masses and then, considering the known masses of the dimer or monomer proteins, the amount of bound detergent and frictional ratio. Data previously published for BmrA and BmrC/BmrD were also analyzed in the same way for comparison (Table 1). In summary, we used two independent ways to determine the association state of PatA, PatB, and PatA/PatB, combining, on one hand, refractive index and light scattering coupled to size exclusion chromatography and, on the other hand, the sedimentation coefficient from AUC and the hydrodynamic radius from SEC. The two methods unambiguously revealed that PatA alone or PatA/PatB contained essentially dimers (∼70%). For PatA/PatB, one cannot distinguish between homo- and/or heterodimers. In contrast, purified PatB contained a mixture of monomers and homodimers.

PatA/PatB Displays a Vanadate-Sensitive ATPase Activity, in Contrast to PatA or PatB Alone. The ATPase activity of the purified proteins, PatA, PatB, and PatA/PatB, was studied. An activity of ∼350 nmol of ATP hydrolyzed min^{-1} (mg of protein)$^{-1}$ was measured for PatA/PatB, and it was inhibited by vanadate [∼80% inhibition (see Figure 5A)]. This

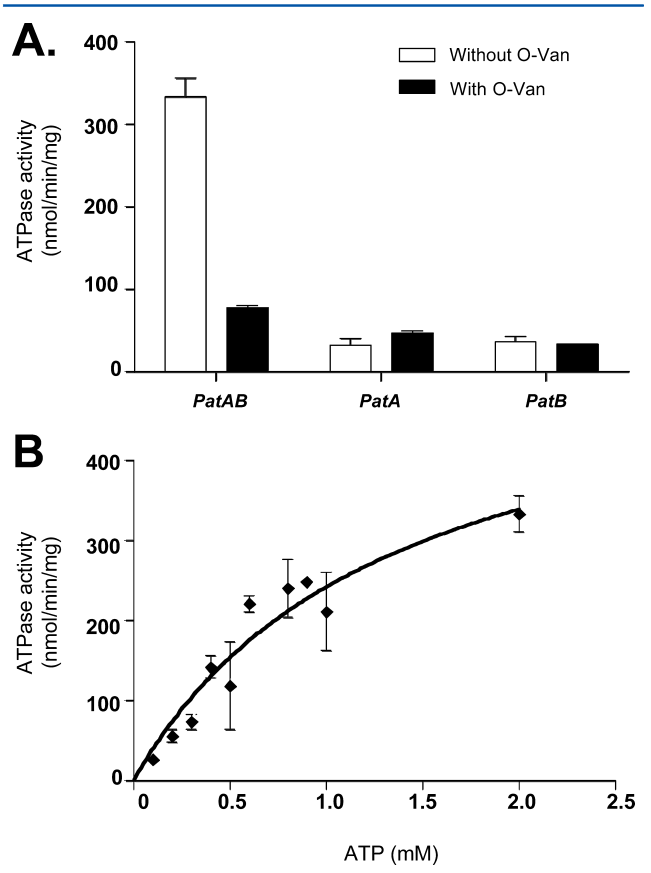

Figure 5. ATPase activities of PatA, PatB, and PatA/PatB and sensitivity to vanadate inhibition. (A) ATPase activities of PatA, PatB, and PatA/PatB purified in the presence of DDM (white bars). Orthovanadate (O-Van, 1 mM) was added before ATP (black bars). (B) Effect of increasing concentrations of ATP on the ATPase activity of purified PatA/PatB. The solid line represents the best fit of the data to a Michaelis−Menten equation (using Grafit 5 from Erithacus). Experiments presented here were repeated at least three times, and the results of one representative experiment are shown here. The error bars represent the SEM for one experiment conducted in triplicate.

dx.doi.org/10.1021/bi300762p | Biochemistry 2012, 51, 7755−7765

inhibition is similar to that found for two related bacterial multidrug ABC transporters solubilized in DDM as well.[34,38] In contrast, the preparations containing either individual protein, PatA or PatB, showed a low ATPase activity (10−15%) that was totally insensitive to vanadate inhibition. Because some ATPases are known to be insensitive to vanadate inhibition,[39−42] the ATPase activity in either the PatA or PatB purified fraction is likely due to some *E. coli* ATPases that contaminated our preparations. A similar conclusion was drawn previously when BmrC and BmrD from *B. subtilis* were purified either jointly or separately using a similar purification protocol like that described here.[34] Last, we determined the kinetic constants for hydrolysis of ATP by PatA/PatB purified in DDM (Figure 5B). Data obtained using increasing ATP concentrations were fit to the Michaelis−Menten equation with a calculated V_{max} of 566.7 ± 100 nmol of ATP hydrolyzed min^{-1} $(mg\ of\ protein)^{-1}$ and a K_M value of 1.3 ± 0.4 mM ATP.

DISCUSSION

On the basis of the genetic evidence using *S. pneumoniae* mutant strains either invalidated in *patA* and/or *patB*[19,23] or upregulated in *patA* and *patB* expression,[20−22,43] PatA and PatB were inferred to form a functional multidrug efflux transporter. Here, we show that PatA and PatB associate as a functional heterodimeric ABC transporter, yet PatA and PatB are rather unconventional half-ABC exporters in the bacterial kingdom, as opposed to other previously characterized bacterial heterodimeric multidrug ABC transporters (e.g., refs 11, 14, and 44) because their encoding genes Spr1885 (*patB*) and Spr1887 (*patA*) are separated by a gene (Spr1886) encoding a putative transposase. The physiological relevance of this latter gene remains an unsettled issue.[20,23] Nevertheless, Spr1885 and Spr1887 belong to the same operon, and their expression or overexpression in the presence of some drugs is tightly coregulated.[20,23]

A puzzling aspect of this transporter is that PatA has been suggested to be functional on its own and therefore to homodimerize to confer resistance to reserpine.[23] However, even though PatA forms a stable homodimer in vitro, we have established that it is neither a functional ATPase nor a xenobiotic transporter. On the contrary, heterodimerization of PatA/PatB is clearly required for drug transport and vanadate-sensitive ATPase activity. PatB alone was isolated as a mixture of nonfunctional dimers and monomers. This suggested that homodimers of PatB are rather unstable per se and that they required their cognate partner, PatA, to remain in a stable functional form. Consequently, this implies that in the PatA/PatB purified fraction, the dimers are mostly, if not exclusively, heterodimers. A similar situation was found for the ABCG5/ABCG8 half-transporters. When overexpressed and purified alone, ABCG8 formed stable homodimers in contrast to ABCG5 that appeared rather unstable, but the overexpression of ABCG5/ABCG8 together allowed the purification of stable and functional heterodimers.[45]

Another possible explanation for the finding by Garvey and Piddock that disruption of PatA alone resulted in the loss of reserpine resistance in a selected strain originally overexpressing both PatA and PatB[23] would be that PatA could heterodimerize with another ABC half-transporter in *S. pneumoniae*. This as yet uncharacterized putative heterodimer (PatA with X) would then be responsible for reserpine resistance. Indeed, several pieces of evidence for promiscuous interactions for some half-ABC transporters have been reported previously.[46,47] For instance, plant ABCG11 has been shown either to homodimerize or to pair with different half-transporters, such as ABCG12, to transport different substrates in different tissues.[48] In contrast, ABCG12 is unable to homodimerize and forms an obligate heterodimer with ABCG11.[48] Among the 78 known and putative ABC proteins present in the *S. pneumoniae* genome (http://www.membranetransport.org/), several encode half-transporters that might be alternative partners of PatA. This includes notably the Spr1656/Spr1657 putative pair in the R6 strain whose related transporter in *B. subtilis* was shown to be a multidrug transporter.[14] If the interaction of PatA with another protein partner were to occur in vivo, this would presumably outcompete the PatA−PatA interaction seen here in vitro in the absence of PatB.

A promiscuous interaction of PatA would also explain why *patB* was found to be dispensable for normal growth either in the R6 or M22 strain, while a *patA* disruption significantly reduced the rate of growth in a R6 background and was very likely unviable in the M22 background.[21] In this report, however, we found no evidence of a growth defect of the Δ*patA* mutant in the R6 background, in agreement with the results of Roberston and colleagues who were able to disrupt the *patA* gene in a TIGR4 strain without any phenotypic consequence.[19] Notwithstanding this discrepancy, several lines of evidence, including the physical association of PatA and PatB shown here, support a role of the PatA/PatB heterodimer as a multidrug transporter responsible for fluoroquinolone resistance in *S. pneumoniae*.

Purification of membrane proteins is a very challenging task and the first bottleneck that must be overcome is the overexpression step. Here a remarkably high level of overexpression of both PatA and PatB was achieved in *E. coli* strain C41(DE3), or in its parental BL21(DE3) strain although in a lower yield (not shown), with a massive incorporation of the two proteins in the membrane fraction. Previously, we overexpressed in high yield two bacterial multidrug ABC transporters with a preference for either the C41(DE3) or the BL21(DE3) strain for BmrA or BmrC/BmrD, respectively.[14,29] Therefore, depending upon the transporter considered and even when they seem closely related, a tuning for the overexpression parameters, including different *E. coli* strains and growth conditions, must be optimized and cannot be generalized a priori. A very high level of overexpression of the heterodimeric multidrug exporter TmrA/TmrB from *Thermus thermophilus* was also reported using *E. coli* strain BL21-(DE3).[44] On the other hand, a nisin inducible promoter using a *Lactococcus lactis* strain was used to overexpress and purify LmrA and LmrC/LmrD,[10,49] but we were also able to overexpress LmrA in *E. coli*.[29] Lately, both *E. coli*- and *L. lactis*-overexpressing systems were used to purify the heterodimeric multidrug exporter TM287/TM288 from *Thermotoga maritima*.[50] However, because of a more efficient overexpression and a reduced cost of purification, the *E. coli* system was preferred to routinely purify and crystallize the transporter (M. Seeger, personal communication), thereby leading to the first high-resolution structure of a heterodimeric multidrug ABC exporter.[50] Although a high level of overexpression could lead to some misfolding of the protein, the correct addressing of the protein to the membrane in addition to the functional test performed here, at the membrane and purified levels, makes it reasonable to assume that the majority of the PatA/PatB heterodimers were overproduced and purified in a native-like state.

AUTHOR INFORMATION

Corresponding Author

*IBS, 41 rue Jules Horowitz, F-38027 Grenoble Cedex 1, France. Telephone: +33 (0)4 38 78 31 19. E-mail: thierry.vernet@ibs.fr (T.V.) or jean-michel.jault@ibs.fr (J.-M.J.).

Present Address

§Plateforme Proteogen, IFR 146 ICORE, Université de Caen Basse-Normandie, Esplanade de la paix, 14032 Caen, France.

Funding

We are indebted to the FINOVI foundation for its financial support of the entire project, including a postdoctoral fellowship to E.B., and we thank the 'Partnership for Structural Biology' in Grenoble for the use of the AUC and PAOL platforms at the IBS.

Notes

The authors declare no competing financial interest.

ACKNOWLEDGMENTS

We thank Dr. Markus Seeger for sharing with us unpublished information about the overexpression of TM287/TM288.

REFERENCES

(1) Bartlett, J. G., and Mundy, L. M. (1995) Community-acquired pneumonia. *N. Engl. J. Med. 333*, 1618−1624.

(2) Van Bambeke, F., Reinert, R. R., Appelbaum, P. C., Tulkens, P. M., and Peetermans, W. E. (2007) Multidrug-resistant *Streptococcus pneumoniae* infections: Current and future therapeutic options. *Drugs 67*, 2355−2382.

(3) Levy, S. B., and Marshall, B. (2004) Antibacterial resistance worldwide: Causes, challenges and responses. *Nat. Med. 10*, S122−S129.

(4) Piddock, L. J. (2006) Clinically relevant chromosomally encoded multidrug resistance efflux pumps in bacteria. *Clin. Microbiol. Rev. 19*, 382−402.

(5) Ren, Q., Chen, K., and Paulsen, I. T. (2007) TransportDB: A comprehensive database resource for cytoplasmic membrane transport systems and outer membrane channels. *Nucleic Acids Res. 35*, D274−D279.

(6) Higgins, C. F. (2007) Multiple molecular mechanisms for multidrug resistance transporters. *Nature 446*, 749−757.

(7) Davidson, A. L., Dassa, E., Orelle, C., and Chen, J. (2008) Structure, function, and evolution of bacterial ATP-binding cassette systems. *Microbiol. Mol. Biol. Rev. 72*, 317−364.

(8) Geourjon, C., Orelle, C., Steinfels, E., Blanchet, C., Deleage, G., Di Pietro, A., and Jault, J. M. (2001) A common mechanism for ATP hydrolysis in ABC transporter and helicase superfamilies. *Trends Biochem. Sci. 26*, 539−544.

(9) Huda, N., Lee, E. W., Chen, J., Morita, Y., Kuroda, T., Mizushima, T., and Tsuchiya, T. (2003) Molecular cloning and characterization of an ABC multidrug efflux pump, VcaM, in Non-O1 Vibrio cholerae. *Antimicrob. Agents Chemother. 47*, 2413−2417.

(10) Lubelski, J., Mazurkiewicz, P., van Merkerk, R., Konings, W. N., and Driessen, A. J. (2004) ydaG and ydbA of *Lactococcus lactis* encode a heterodimeric ATP-binding cassette-type multidrug transporter. *J. Biol. Chem. 279*, 34449−34455.

(11) Margolles, A., Florez, A. B., Moreno, J. A., van Sinderen, D., and de los Reyes-Gavilan, C. G. (2006) Two membrane proteins from *Bifidobacterium breve* UCC2003 constitute an ABC-type multidrug transporter. *Microbiology (Reading, U.K.) 152*, 3497−3505.

(12) Sakamoto, K., Margolles, A., van Veen, H. W., and Konings, W. N. (2001) Hop resistance in the beer spoilage bacterium *Lactobacillus brevis* is mediated by the ATP-binding cassette multidrug transporter HorA. *J. Bacteriol. 183*, 5371−5375.

(13) Steinfels, E., Orelle, C., Fantino, J. R., Dalmas, O., Rigaud, J. L., Denizot, F., Di Pietro, A., and Jault, J. M. (2004) Characterization of YvcC (BmrA), a Multidrug ABC Transporter Constitutively Expressed in *Bacillus subtilis*. *Biochemistry 43*, 7491−7502.

(14) Torres, C., Galian, C., Freiberg, C., Fantino, J. R., and Jault, J. M. (2009) The YheI/YheH heterodimer from *Bacillus subtilis* is a multidrug ABC transporter. *Biochim. Biophys. Acta 1788*, 615−622.

(15) van Veen, H. W., Venema, K., Bolhuis, H., Oussenko, I., Kok, J., Poolman, B., Driessen, A. J., and Konings, W. N. (1996) Multidrug resistance mediated by a bacterial homolog of the human multidrug transporter MDR1. *Proc. Natl. Acad. Sci. U.S.A. 93*, 10668−10672.

(16) Raherison, S., Gonzalez, P., Renaudin, H., Charron, A., Bebear, C., and Bebear, C. M. (2005) Increased expression of two multidrug transporter-like genes is associated with ethidium bromide and ciprofloxacin resistance in *Mycoplasma hominis*. *Antimicrob. Agents Chemother. 49*, 421−424.

(17) Lee, E. W., Huda, M. N., Kuroda, T., Mizushima, T., and Tsuchiya, T. (2003) EfrAB, an ABC multidrug efflux pump in *Enterococcus faecalis*. *Antimicrob. Agents Chemother. 47*, 3733−3738.

(18) Lubelski, J., Konings, W. N., and Driessen, A. J. (2007) Distribution and Physiology of ABC-Type Transporters Contributing to Multidrug Resistance in Bacteria. *Microbiol. Mol. Biol. Rev. 71*, 463−476.

(19) Robertson, G. T., Doyle, T. B., and Lynch, A. S. (2005) Use of an efflux-deficient *Streptococcus pneumoniae* strain panel to identify ABC-class multidrug transporters involved in intrinsic resistance to antimicrobial agents. *Antimicrob. Agents Chemother. 49*, 4781−4783.

(20) Feng, J., Lupien, A., Gingras, H., Wasserscheid, J., Dewar, K., Legare, D., and Ouellette, M. (2009) Genome sequencing of linezolid-resistant *Streptococcus pneumoniae* mutants reveals novel mechanisms of resistance. *Genome Res. 19*, 1214−1223.

(21) Marrer, E., Schad, K., Satoh, A. T., Page, M. G., Johnson, M. M., and Piddock, L. J. (2006) Involvement of the putative ATP-dependent efflux proteins PatA and PatB in fluoroquinolone resistance of a multidrug-resistant mutant of *Streptococcus pneumoniae*. *Antimicrob. Agents Chemother. 50*, 685−693.

(22) Garvey, M. I., Baylay, A. J., Wong, R. L., and Piddock, L. J. (2011) Overexpression of patA and patB, which encode ABC transporters, is associated with fluoroquinolone resistance in clinical isolates of *Streptococcus pneumoniae*. *Antimicrob. Agents Chemother. 55*, 190−196.

(23) Garvey, M. I., and Piddock, L. J. (2008) The efflux pump inhibitor reserpine selects multidrug-resistant *Streptococcus pneumoniae* strains that overexpress the ABC transporters PatA and PatB. *Antimicrob. Agents Chemother. 52*, 1677−1685.

(24) Miroux, B., and Walker, J. E. (1996) Over-production of proteins in *Escherichia coli*: Mutant hosts that allow synthesis of some membrane proteins and globular proteins at high levels. *J. Mol. Biol. 260*, 289−298.

(25) Fadda, D., Pischedda, C., Caldara, F., Whalen, M. B., Anderluzzi, D., Domenici, E., and Massidda, O. (2003) Characterization of divIVA and other genes located in the chromosomal region downstream of the dcw cluster in *Streptococcus pneumoniae*. *J. Bacteriol. 185*, 6209−6214.

(26) Claverys, J. P., Dintilhac, A., Pestova, E. V., Martin, B., and Morrison, D. A. (1995) Construction and evaluation of new drug-resistance cassettes for gene disruption mutagenesis in *Streptococcus pneumoniae*, using an ami test platform. *Gene 164*, 123−128.

(27) Guiral, S., Henard, V., Laaberki, M. H., Granadel, C., Prudhomme, M., Martin, B., and Claverys, J. P. (2006) Construction and evaluation of a chromosomal expression platform (CEP) for ectopic, maltose-driven gene expression in *Streptococcus pneumoniae*. *Microbiology (Reading, U.K.) 152*, 343−349.

(28) Bayle, L., Chimalapati, S., Schoehn, G., Brown, J., Vernet, T., and Durmort, C. (2011) Zinc uptake by *Streptococcus pneumoniae* depends on both AdcA and AdcAII and is essential for normal bacterial morphology and virulence. *Mol. Microbiol. 82*, 904−916.

(29) Steinfels, E., Orelle, C., Dalmas, O., Penin, F., Miroux, B., Di Pietro, A., and Jault, J. M. (2002) Highly efficient over-production in *E. coli* of YvcC, a multidrug-like ATP-binding cassette transporter from *Bacillus subtilis*. *Biochim. Biophys. Acta 1565*, 1−5.

(30) Schuck, P. (2000) Size-distribution analysis of macromolecules by sedimentation velocity ultracentrifugation and Lamm equation modeling. *Biophys. J. 78*, 1606−1619.
(31) Ebel, C. (2011) Sedimentation velocity to characterize surfactants and solubilized membrane proteins. *Methods (San Diego, CA, U.S.) 54*, 56−66.
(32) le Maire, M., Arnou, B., Olesen, C., Georgin, D., Ebel, C., and Moller, J. V. (2008) Gel chromatography and analytical ultracentrifugation to determine the extent of detergent binding and aggregation, and Stokes radius of membrane proteins using sarcoplasmic reticulum Ca^{2+}-ATPase as an example. *Nat. Protoc. 3*, 1782−1795.
(33) Salvay, A. G., Santamaria, M., le Maire, M., and Ebel, C. (2007) Analytical Ultracentrifugation Sedimentation Velocity for the Characterization of Detergent-Solubilized Membrane Proteins Ca^{2+}-ATPase and ExbB. *J. Biol. Phys. 33*, 399−419.
(34) Galian, C., Manon, F., Dezi, M., Torres, C., Ebel, C., Levy, D., and Jault, J. M. (2011) Optimized purification of a heterodimeric ABC transporter in a highly stable form amenable to 2-D crystallization. *PLoS One 6*, e19677.
(35) Jault, J. M., Di Pietro, A., Falson, P., and Gautheron, D. C. (1991) Alteration of apparent negative cooperativity of ATPase activity by α-subunit glutamine 173 mutation in yeast mitochondrial F1. Correlation with impaired nucleotide interaction at a regulatory site. *J. Biol. Chem. 266*, 8073−8078.
(36) Shapiro, A. B., Corder, A. B., and Ling, V. (1997) P-Glycoprotein-mediated Hoechst 33342 transport out of the lipid bilayer. *Eur. J. Biochem. 250*, 115−121.
(37) Shapiro, A. B., and Ling, V. (1997) Positively cooperative sites for drug transport by P-glycoprotein with distinct drug specificities. *Eur. J. Biochem. 250*, 130−137.
(38) Ravaud, S., Do Cao, M. A., Jidenko, M., Ebel, C., Le Maire, M., Jault, J. M., Di Pietro, A., Haser, R., and Aghajari, N. (2006) The ABC transporter BmrA from *Bacillus subtilis* is a functional dimer when in a detergent-solubilized state. *Biochem. J. 395*, 345−353.
(39) Hicks, D. B., and Krulwich, T. A. (1986) The membrane ATPase of alkalophilic *Bacillus firmus* RAB is an F1-type ATPase. *J. Biol. Chem. 261*, 12896−12902.
(40) Rees-Jones, R., and Al-Awqati, Q. (1984) Proton-translocating adenosinetriphosphatase in rough and smooth microsomes from rat liver. *Biochemistry 23*, 2236−2240.
(41) Laubinger, W., and Dimroth, P. (1987) Characterization of the Na^+-stimulated ATPase of *Propionigenium modestum* as an enzyme of the F1F0 type. *Eur. J. Biochem. 168*, 475−480.
(42) Sarkadi, B., Price, E. M., Boucher, R. C., Germann, U. A., and Scarborough, G. A. (1992) Expression of the human multidrug resistance cDNA in insect cells generates a high activity drug-stimulated membrane ATPase. *J. Biol. Chem. 267*, 4854−4858.
(43) Marrer, E., Satoh, A. T., Johnson, M. M., Piddock, L. J., and Page, M. G. (2006) Global transcriptome analysis of the responses of a fluoroquinolone-resistant *Streptococcus pneumoniae* mutant and its parent to ciprofloxacin. *Antimicrob. Agents Chemother. 50*, 269−278.
(44) Zutz, A., Hoffmann, J., Hellmich, U. A., Glaubitz, C., Ludwig, B., Brutschy, B., and Tampe, R. (2011) Asymmetric ATP hydrolysis cycle of the heterodimeric multidrug ABC transport complex TmrAB from *Thermus thermophilus*. *J. Biol. Chem. 286*, 7104−7115.
(45) Wang, Z., Stalcup, L. D., Harvey, B. J., Weber, J., Chloupkova, M., Dumont, M. E., Dean, M., and Urbatsch, I. L. (2006) Purification and ATP hydrolysis of the putative cholesterol transporters ABCG5 and ABCG8. *Biochemistry 45*, 9929−9939.
(46) Liu, L. X., Janvier, K., Berteaux-Lecellier, V., Cartier, N., Benarous, R., and Aubourg, P. (1999) Homo- and heterodimerization of peroxisomal ATP-binding cassette half-transporters. *J. Biol. Chem. 274*, 32738−32743.
(47) Genin, E. C., Geillon, F., Gondcaille, C., Athias, A., Gambert, P., Trompier, D., and Savary, S. (2011) Substrate specificity overlap and interaction between adrenoleukodystrophy protein (ALDP/ABCD1) and adrenoleukodystrophy-related protein (ALDRP/ABCD2). *J. Biol. Chem. 286*, 8075−8084.
(48) McFarlane, H. E., Shin, J. J., Bird, D. A., and Samuels, A. L. (2010) *Arabidopsis* ABCG transporters, which are required for export of diverse cuticular lipids, dimerize in different combinations. *Plant Cell 22*, 3066−3075.
(49) Margolles, A., Putman, M., van Veen, H. W., and Konings, W. N. (1999) The purified and functionally reconstituted multidrug transporter LmrA of *Lactococcus lactis* mediates the transbilayer movement of specific fluorescent phospholipids. *Biochemistry 38*, 16298−16306.
(50) Hohl, M., Briand, C., Grutter, M. G., and Seeger, M. A. (2012) Crystal structure of a heterodimeric ABC transporter in its inward-facing conformation. *Nat. Struct. Mol. Biol. 19*, 395−402.